PAPER

Local electrochemical control of hydrogel microactuators in microfluidics

IOP Publishing Journal of Micromechanics and Microengineering
J. Micromech. Microeng. **28** (2018) 105005 (9pp) https://doi.org/10.1088/1361-6439/aacc31

Local electrochemical control of hydrogel microactuators in microfluidics

Leeya Engel[1], Chengming Liu[2], Nofar Mintz Hemed[3], Yasser Khan[2], Ana Claudia Arias[2], Yosi Shacham-Diamand[3], Slava Krylov[4] and Liwei Lin[5]

[1] Department of Biongineering, Stanford University, Stanford, CA, 94305, United States of America
[2] Department of Electrical Engineering and Computer Sciences, University of California, Berkeley, Berkeley 94720, CA, United States of America
[3] Faculty of Engineering, School of Electrical Engineering, Tel Aviv University, Ramat Aviv 69978, Israel
[4] Faculty of Engineering, School of Mechanical Engineering, Tel Aviv University, Ramat Aviv 69978, Israel
[5] Department of Mechanical Engineering, University of California, Berkeley, Berkeley 94720, CA, United States of America

E-mail: Leeya@stanford.edu

Received 8 March 2018, revised 29 May 2018
Accepted for publication 13 June 2018
Published 29 June 2018

Abstract

Due to the complexity of a chemo-electro-mechanical system and the need for a wet environment, to date, few devices fully integrate hydrogels with microelectromechanical systems. In this paper, we demonstrate the use of inkjet-printed gold electrodes integrated in microfluidic channels to alter the morphology of electroactive polymer hydrogels, cross-linked *in situ*. Microfluidics is a convenient platform for integrating hydrogels with microsystems as it provides a means for encapsulating electrolytic environments, while maintaining UV transparency. Printed electronics provide a new method for rapid prototyping of electrodes on flexible substrates for electrical control of electroactive polymer microsystems. We attribute the observed actuation to electrochemically-induced pH variations in the vicinity of the printed anode and cathode which diffuse into the hydrogel. Response to pH was verified by exposing the hydrogel to various pH conditions in control experiments without applied electrical bias. This work demonstrates a new, integrated, polymer-based, rapid prototyping approach to building flexible electroactive hydrogel systems which can benefit microfluidic valves, biomimetics, electrochemical sensors and artificial muscles.

Keywords: electroresponsive hydrogel, polyelectrolyte hydrogel, electroactive polymers, printed electrodes, polymer MEMS, hydrogel actuator, artificial muscles

(Some figures may appear in colour only in the online journal)

1. Introduction

Polyelectrolyte hydrogels, electrically stimulated in salt solution, are a class of electroactive polymers (EAPs) that have been widely researched in recent years for their applications in biomimetics [1, 2], drug delivery, tissue engineering [3, 4], implantation [5] and soft robotics [6–8]. Despite the potential of EAP hydrogels to function as active elements in microfluidics-based diagnostic and therapeutic tools, or as artificial muscles, they have been considered less suitable than field-activated EAPs for implementation in microsystems for their comparatively low efficiency, low actuation forces, and slow response times [9], which have mainly limited their industrial applications to drug delivery systems.

The general mechanism of actuation in EAP hydrogel systems is change of dimension in response to electrically-induced osmotic concentration gradients [10]. EAP hydrogels that are stimulated electrostatically in electrolytic environments experience coupled chemical, electrical, and mechanical fields, and are thus challenging to model [11]. Deformation of

pH-sensitive hydrogels in microfluidic systems, however, has been modeled by He *et al* [12]. The sensitivity of polyelectrolyte hydrogels to a host of experimental parameters (i.e. pH, temperature, ionic concentration of solution, concentration of fixed charges) that vary between experimental works (i.e. hydrogel composition, magnitude of potential difference between electrodes, distance between electrodes and sample) makes it difficult to compare data from different studies.

It is the challenge of integration with electronics that presents the biggest impediment to implementing EAP hydrogels in microsystems. While electrical stimulation of EAP hydrogels via integrated circuits could allow for an unprecedented degree of control over EAP hydrogel expansion/contraction, most conventional metals used in microsystems are not electrochemically stable. Electrochemical related corrosion of electrodes can significantly influence biocompatibility and performance of microelectromechanical systems (MEMS) controlled by microelectronics and must be characterized in an electrolytic context before they can be applied to the stimulation of EAP hydrogels.

Response times of hydrogel actuators can be drastically reduced by downscaling hydrogel actuators [13], creating shorter diffusion paths that ions and solution must traverse in and out of the polymer matrix to effect change of dimension in the sample. The recent trend of using photopolymerization for hydrogel synthesis allows for good spatial and temporal control over gelation [14] and is key for downscaling hydrogel actuator systems. A review of the synthesis, characteristics, and applications of microscale hydrogels for medicine and biology by Rivest *et al* shows two main ways for downscaling hydrogel systems: photolithography and micromolding [3]. Integration with microsystems is compatible with the former method, as microfluidics, together with optofluidic lithography through UV-transparent channels, has been established as a means for fabricating small-scale hydrogel structures inside encapsulated electrolytic environments. Examples of these systems include pH or temperature responsive microvalves [15–18] and multifunctional soft mini aquabots that mimic sperm, octopus, and myriapod locomotion [19].

In EAP hydrogel systems, macroscale plate or wire electrodes are typically used to provide electrical stimulation [5, 10, 16, 18–22]. These are challenging to integrate with microfluidics and cannot be patterned, making it difficult to explore the response of the EAP hydrogels as a function of electrode configuration. Jackson *et al* reported that electrode wire configuration was a significant factor in controlling radial deswelling of cylindrical EAP hydrogel samples synthesized for implantation [20]. A smaller scale, integrated MEMS platform for characterization of stimuli-sensitive hydrogels was fabricated and tested by Guan *et al* using chromium electrodes for sensing, but this fabrication scheme required multiple masks and lithography steps [23].

Printed electrodes integrated with microfluidics would allow for rapid prototyping of a variety of electrode configurations, as compared to electrodes patterned by optical lithography, which require additional masks for new designs, significantly increasing design iteration time. Currently, printed circuits are used in a range of applications, including organic thin-film transistors, light-emitting diodes, solar cells, sensors, and biological/pharmaceutical tasks [24–26]. However, despite significant progress in printing technology, there remain significant hurdles in integrating printed circuitry and microfluidics, likely due to two primary limitations: (i) electrochemical instability of the printed electrodes, and (ii) incompatibility of heat-sensitive substrates due to post-printing sintering and the need to remove volatile components in the ink such as excess solvent and organic stabilizers [25].

In this paper, we demonstrate a fully integrated downscaled EAP hydrogel device, fabricated by integrating printed electrodes within a microfluidic channel and performing *in situ* photopolymerization to micropattern EAP hydrogel structures. We propose an explanation for the mechanism causing morphological changes to the crosslinked hydrogel in response to the electrical stimulation via printed circuits. This rapid, lost-cost fabrication scheme and integrated EAP system establishes a platform for exploring the response of hydrogels to electrical stimulation in biologically-relevant solutions, and probing the role of electrode configuration in the mechanical response of EAP hydrogels.

2. Materials and methods

A schematic sketch of our experimental setup is shown in figure 1. The process flow is summarized in figure 2.

2.1. Electrode fabrication

Flexible electrodes were inkjet printed on top of a thin (25 μm thick) planarized polyethylene naphthalate (PEN) substrate (DuPont). Harima gold nano-paste ink (model: NPG-J) was inkjet printed using a Dimatix Materials Printer (DMP-2800) with 30 μm drop spacing. A sintering process was then performed in air by annealing the wet printed electrodes from 30 °C to 200 °C with a 30 °C min^{-1} ramp, followed by a baking at a constant temperature of 200 °C for 60 min. This anneal step evaporates the solvents from the printed structures and displaces the surfactants from the surfaces of the gold (Au) nanoparticles, stabilizing and reducing the resistance of the sintered electrodes [27, 28]. Following annealing, we measured the resistance of the printed electrodes using a multimeter connected to a probe station.

2.2. Electrochemical characterization

Electrochemical impedance spectroscopy (EIS) and cyclic-voltammetry (CV) were performed in a conventional three-electrode electrochemical cell comprised of the Au printed electrode as a working electrode, platinum (Pt) wire as a counter electrode, and a homemade open Ag/AgCl reference electrode made by Ag plating followed by anodization in a chlorine salt solution. Stability of the Ag/AgCl reference electrode was studied versus commercial Ag/AgCl (Saturated KCl) electrodes and was found to be stable with very low drift in standard phosphate buffer (PB). CV measurements were performed over a voltage sweep of $\pm$2.5 V with a scan rate of

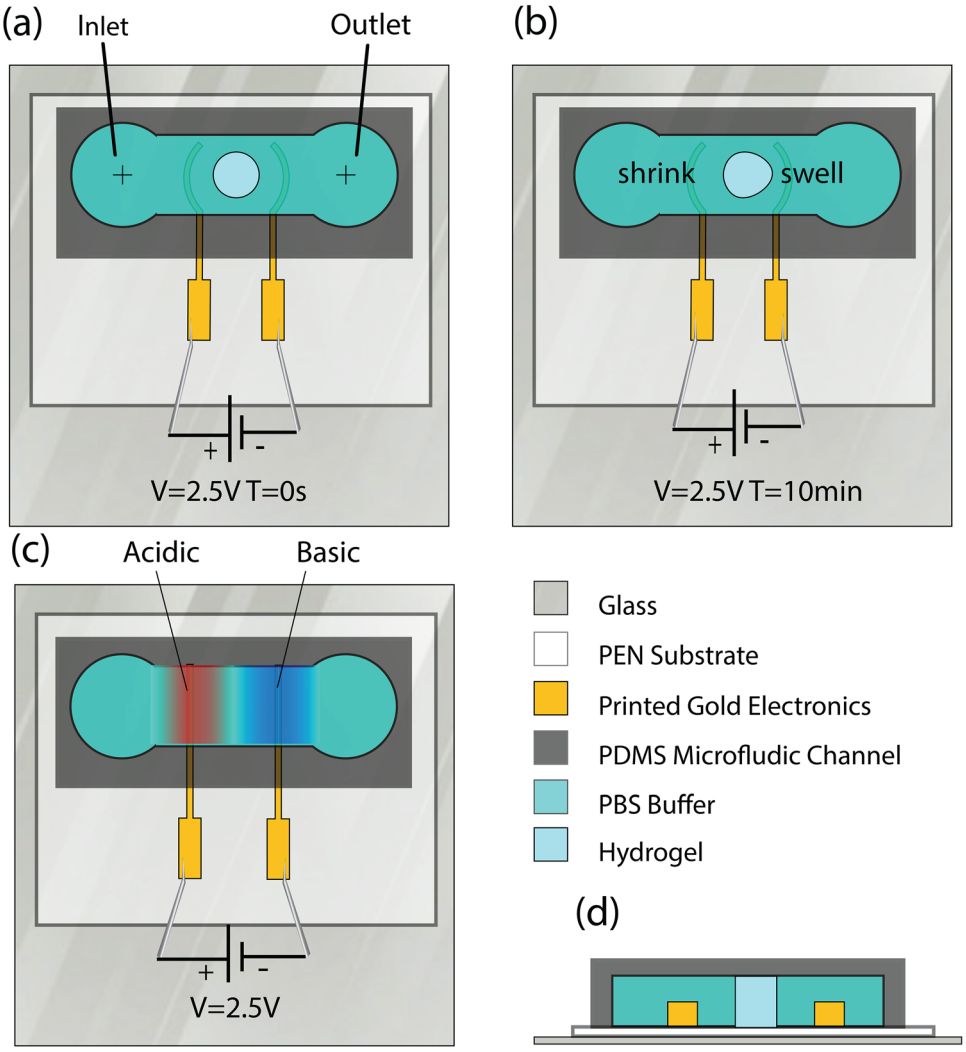

Figure 1. A crosslinked anionic hydrogel sample in a microfluidic channel with integrated Au electrodes. (a) Before application of voltage. (b) Following application of potential difference, circle becomes asymmetric due to swelling at contraction at either side of sample. (c) pH waves emanate from electrodes during application of an electrical signal. (d) Cross-sectional view of setup.

0.05 V s^{-1} for 40 cycles. The electrolyte used was PB, with pH adjusted to 5.9, 7.2 and 7.9 at room temperature. For selected electrodes EIS was performed at a frequency range of 0.1 Hz–200 kHz, under open circuit potential with 10 mV modulation voltage, using potentiostat/galvanostat (VSP, BioLogic science instruments Ltd.).

2.3. Microfluidic channel fabrication

Fabrication of the PDMS channels followed previous works [29], with an added challenge of adhering the PDMS slab containing the channels to the sheet of PEN on which the electrodes were printed, rather than to a glass surface (see figure 3(b)). To bond the PDMS channels to the PEN with the electrodes, we exposed the PDMS and PEN surfaces to UV ozone treatment (UVO cleaner, model 42, Jetlight Company, Irvine, CA) for 30 min, followed by manually applying additional uncured PDMS to the perimeter of the device. The device was then heated for 1 h at 80 °C on a hotplate to improve the seal. This additional PDMS on the device, which was necessary to seal the PDMS to the PEN, had the consequence of adding height to the channel, resulting in inconsistent channel heights. The PDMS channel with integrated printed electrodes maintained flexibility and was mounted on glass purely for convenience of handling (see figure 3(c)).

2.4. In situ hydrogel synthesis

Monomer solutions used for optofluidics, were comprised of: 2-Hydroxyethyl methacrylate (HEMA), 2-Dimethylaminoethyl methacrylate (DMAEMA), Acrylic Acid (AA), and Ethylene Glycol dimethacrylate (EGDMA) (all from Sigma Aldrich). An anionic monomer solution was made from AA and HEMA in a 1–4 molar ratio (10 g AA, 72.2 g HEMA) with 1% EGDMA and 3% Irgacure by weight. A cationic monomer solution was made from DMAEMA and HEMA in a 1–4 molar ratio (10 g DMAEMA, 33 g HEMA) with 1.4%wt EGDMA and 3%wt Irgacure.

For UV curing of the anionic hydrogels, monomer solutions were injected into PDMS channels, exposed under a

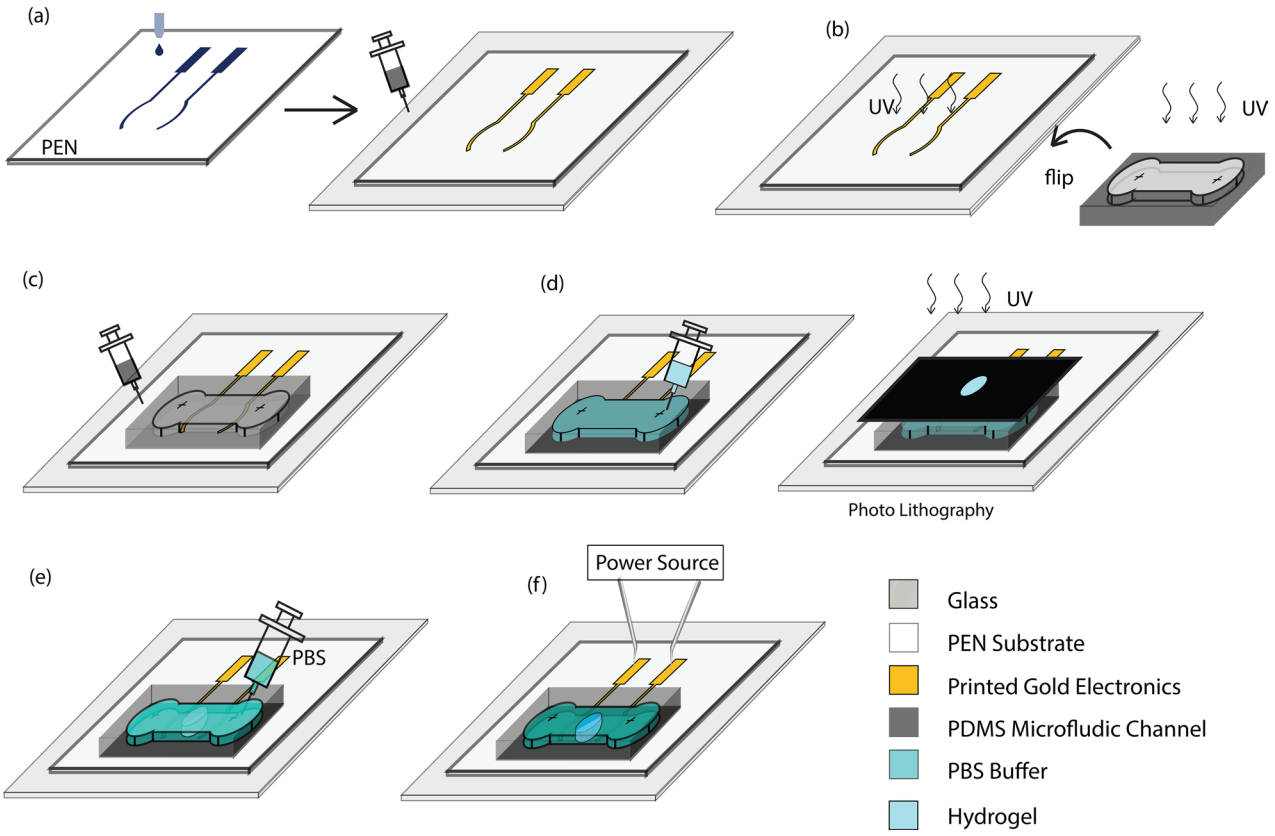

Figure 2. Process flow for fabricating device. (a) Au electrodes are inkjet printed onto PEN. PEN substrate is bonded to thin microscope glass by curing a layer of PDMS between the substrates to ease handling of the device. (b) PDMS channel is bonded to PEN by exposing boding surface of PDMS and PEN to UV light at 100% power for 30 min, followed by an annealing process of heating the device on a hot plate for 1 h at 80 °C. (c) Additional uncured PDMS is applied to the perimeter of the device, followed by an annealing process to improve the seal. (d) Hydrogel prepolymer solution is injected into the empty microfluidic channel, followed by photolithography. (e) Channel is fully flushed with PBS buffer to rinse off any remaining prepolymer solution. (f) Power source is connected to the printed Au electrodes and potential difference is applied to simulate the hydrogel.

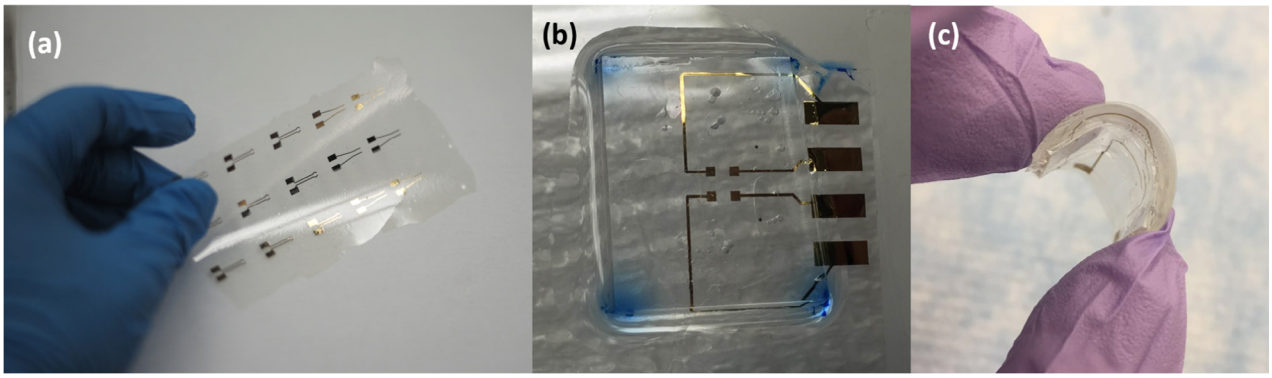

Figure 3. Electrode fabrication. (a) Gold electrodes were printed on PEN. (b) Electrodes were integrated into microfluidic channels. (c) The electroded channels maintained flexibility.

printed mask (Fine Line Imaging, Colorado Springs, CO, USA), and rinsed in phosphate buffer solution (PBS). We verified the sensitivity of the crosslinked samples to changes in pH by flushing the channel with solutions of KOH and H_2SO_4 and recorded the swelling behavior of the gel samples. For these experiments, exposure of the hydrogel prepolymer solution in the channel was performed through the glass slide on which the PDMS channel was mounted using UV light with power of 3.5 mW cm^{-2}, applied for 200 s. To examine reversibility of deformation due to pH variations, we cyclically changed the pH of the environment of one sample.

To crosslink hydrogel samples in channels that contain electrodes printed on PEN, we exposed the solution through the top of the PDMS channel because PEN is not UV transparent. This required us to increase the power of the UV to 7.5 mW cm^{-2}. In all cases, before experiments were performed, the crosslinked hydrogel samples were allowed to reach equilibrium in PBS.

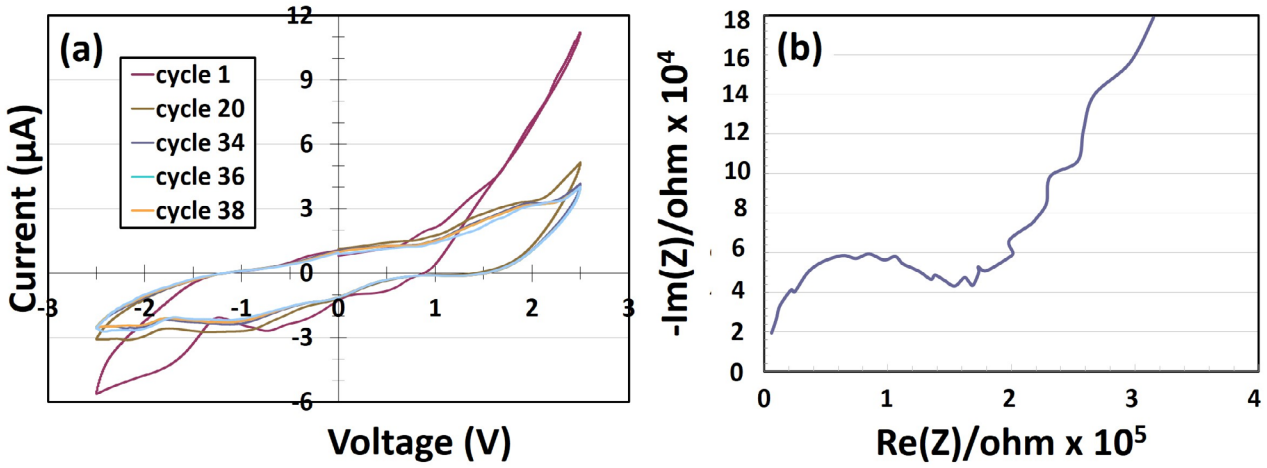

Figure 4. Electrochemical characterization of Au electrodes printed on PEN in PB at neutral pH. (a) IV curves for cyclic voltammetry. No major peaks are observed throughout the test. (b) Electrochemical impedance spectroscopy of inkjet-printed Au electrodes.

2.5. Electrical stimulation

Sample deformation in an EAP hydrogel testing system can be caused by various stimuli (i.e. temp, pH, current, electrical bias), and it can be difficult to isolate the driving force behind observed deformation of a hydrogel sample in a given system [22]. In the current experimental setup, the close proximity of the electrodes to the hydrogel samples makes it important to consider electrochemical reactions taking place at the electrodes and their role in the redistribution of ions in the solution surrounding the hydrogel samples upon the application of a bias in the media, which caused them to deform.

Local pH changes occur in PBS due to the reactions taking place at the electrodes. Specifically, the half reaction that takes place at the anode, $2H_2O \longrightarrow O_2 + 4H^+ + 4e^-$, increases the local concentration of hydronium ions, H_3O^+, resulting in a lower local pH, while the half reaction at the cathode, $2H_2O + 2e^- \longrightarrow H_2 + 2OH^-$, increases the local concentration of hydroxide ions, HO^-, resulting in a higher local pH in the immediate vicinity of the cathode which begins to diffuse outward [30]. Additionally, because KCl is present in PBS solutions, there may be chlorine evolution taking place simultaneously at the anode according to the equation $2Cl^- \longrightarrow Cl_2 + 2e^-$ [31, 32], making the reduction of pH at the anode less acute than in the case of pure water.

The PDMS channel was fully flushed with PBS 0.1 M before the application of electrical stimulation. Au electrodes served as anode and cathode and were probed with curved copper wire instead of sharp tungsten needles to prevent puncture of the PEN film and damage to the Au electrodes. The copper wires were connected to the ground and positive output of a DC voltage source. Constant DC Voltage of 2.5 V was applied to actuate the hydrogel.

3. Results and discussion

3.1. Characterization of printed electrodes

Both electrical and electrochemical characterization of the printed electrodes were performed. The electrodes were characterized electrically before integration into the microfluidic channel. The electrodes demonstrated resistivity of 1.4×10^{-7} Ωm, with a standard deviation of 2.4×10^{-8} Ωm, which is ≈17% of bulk gold's conductivity and is comparable to reported printed gold electrodes used for bioelectronic interfaces [27]. Since non-uniform heating directly correlates to non-uniformities in the resistances of the printed electrodes, we secured the substrate on the hot plate such that the wet ink received uniform heating during the sintering step. After visual, optical, and electrical characterization, the printed electrodes were integrated into the microfluidic device.

The electrodes were examined electrochemically under three different pH conditions: basic, 7.9, acidic, 5.9, and neutral, 7.2. Figure 4(a) shows CV measurements at a pH of 7.2, which indicate stability of the electrodes. Because the electrodes showed similarly stable behavior at a pH of 7.9 (not shown), we infer that the Au printed electrodes are stable in the pH range of 7.2–7.9. During CV measurements performed in the low pH range, around 5.9, we observed instability at reverse bias during all cycles and a loss of Au from the surface of the PEN. For selected electrodes, impedance measurements were performed, and these followed the Randles circuit model (see figure 4(b)) [33].

3.2. EAP hydrogel stimulation

In situ photolithography of both anionic and cationic polyelectrolyte gels was successfully performed inside the PDMS channels. Exposure time was calibrated for each of the monomer solutions until resolutions of tens of microns was achieved (see figure 5). Following this, we performed experiments only on the anionic hydrogel.

We verified that the anionic crosslinked hydrogel samples are pH responsive. Crosslinked P(AA-HEMA) circles 1 mm in diameter swelled by an average of 120.8% in area in basic 1M KOH solution, as observed from above through a microscope. The same samples, after being rinsed in PBS and returning to their original dimensions, shrank by an average of 9.4% area in acidic 1M H_2SO_4 solution. The most drastic change in

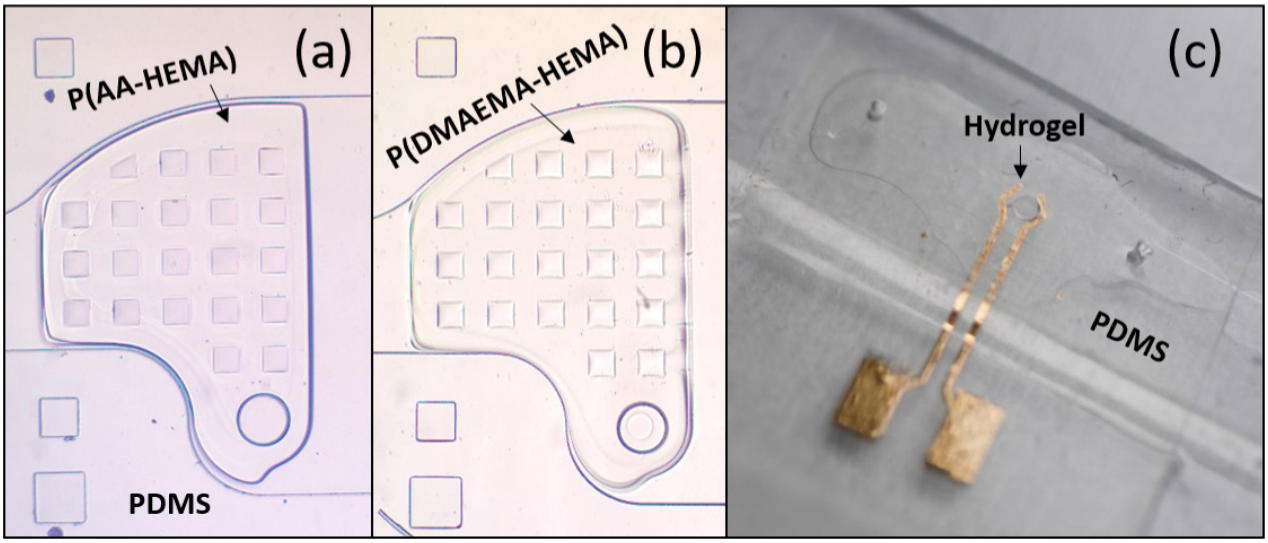

Figure 5. Polyelectrolyte hydrogel structures constructed via *in situ* photolithography in PDMS channels. Crosslinked hydrogel shapes anchored to PDMS posts: (a) anionic and (b) cationic hydrogel. (c) Anionic hydrogel circle with 1 mm in diameter crosslinked between printed Au electrodes.

dimension occurred during the first two minutes of introduction of solution into the channel. For the basic solution, the rate of aerial increase of the hydrogel circle was 38.5% min^{-1} during the first two minutes, and then decreased to 5.4% min^{-1} for the next two minutes. For the acidic solution, the rate of deswelling was 2.9% min^{-1} for the first two minutes, followed by 0.9% for the following two minutes. The rate of change is dependent on a number of parameters such as the ionic strength of the solution and the volume and configuration of the hydrogel sample because the phenomenon of pH-responsivity is governed by diffusion. For example, in figure 6(b), introduction of 2M KOH solution to cross-linked hydrogel features that are 200 μm wide, resulted in a fully swollen state at T_4 on the order of tens of seconds. At times T_1–T_3 a border between the area the basic solution has diffused into and the original, denser hydrogel, that has not yet been affected by the change in pH can be seen. This mismatch in expansion leads to internal stress and buckling of the expanded hydrogel around the perimeter of the samples that later relaxes as the basic solution penetrates the center of the sample.

When we changed the pH in a cyclical way (see figure 6(a)), we observed repeatable swelling and shrinkage of the samples, but also hysteresis. Going from basic solution to neutral PBS resulted in a higher area than when we rinsed hydrogel samples that had been equilibrated in acidic solution with PBS. This hysteresis is likely due to carboxyl bond dissociation in basic solution that does not fully recover upon rinsing in neutral PBS.

We observed morphological changes to circular hydrogel samples in response to an electrical DC voltage applied across the Au printed electrodes. Deformation of a 1 mm in diameter circular hydrogel structures as a function of time in response to 2.5 V DC bias can be seen in figure 7. For the first 4–5 min of bias, the hydrogel on the cathode side continuously expands while the hydrogel on anode side shrinks. After the application of bias, and flushing the channel with PBS, the samples recover their circular shape, thus the actuation is reversible. We did not explore shrinkage or swelling of the sample out of plane, although it is suggested by the observable boundary that develops in the center of the sample as seen via a microscope from above.

In contrast to the dynamic enrichment/depletion mechanism described by Doi *et al* [10] and modeled by Wallmersperger *et al* [11], we hypothesize that the actuation mechanism observed in the current system is electrochemical. Specifically, the hydrogel circle deforms due to local pH changes induced by reduction and oxidation of water taking place at the electrodes. The left electrode in figure 7 functions as a cathode, reducing water to create a basic environment, ionizing carboxyl groups in the hydrogel which then swells due to electrostatic repulsion between negative fixed charges. At the opposite side of the gel, near the anode, hydroxide ions diffuse out of the gel to recombine with hydronium ions in the locally acidic environment, and the gel shrinks. In the current mesoscale setup, the electrodes are in the immediate vicinity of the hydrogel samples and the total volume of liquid is small, implying that the hydrogel sample should immediately be effected by ion evolution taking place at the electrodes.

Electrochemical actuation was ruled out as the primary, or initial, cause for gel bending in systems where macroscale electrodes were placed centimeters away from an EAP hydrogel sample. Electrochemical actuation was, however, observed in these same experimental systems once sufficient time had passed for the change in pH to diffuse from the electrodes to the gel samples [21, 22] and in an experimental setup where two electrodes were in direct contact with a polyelectrolyte hydrogel sample during the electrical stimulation [34, 35]. Although smaller in scale, our results are consistent with these reports.

We tried to directly demonstrate pH changes at the printed Au electrodes using universal pH indicator as has been performed in the literature for Pt [21, 22] and aluminum [34] electrodes in salt solutions, however, due to the small volume of liquid in the channel, the color change was not clearly

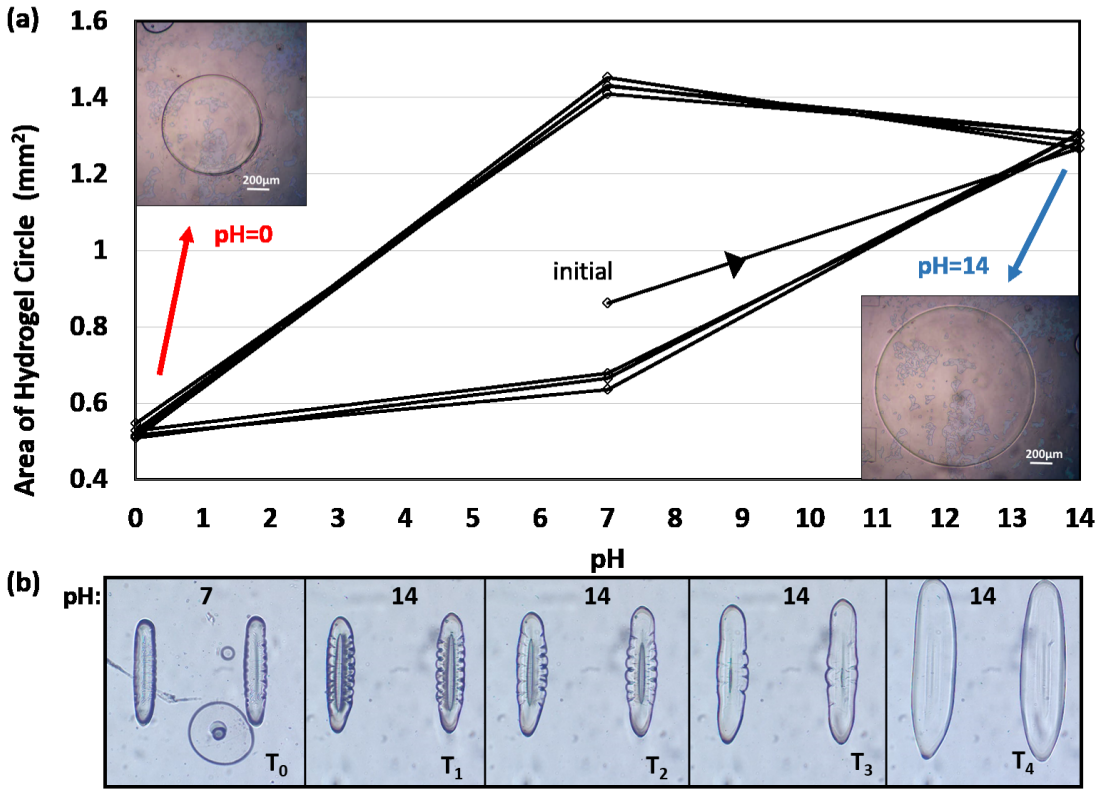

Figure 6. pH response of P(AA-HEMA) structures crosslinked in microfluidic channels. (a) Area of hydrogel circle changes as a function of pH. Circle is 1 mm diameter equilibrium in PBS. Upper inset shows 63.3% decrease in area when exposed to 1M H_2SO_4 (pH = 0). The lower right inset shows the same circle in 1M KOH (pH = 14), where the area increases by 74.4% relative to diameter in PBS. (b) Hydrogel beams 200 μm in width initially equilibriated in PBS at T_0 swell over tens of seconds upon the introduction 2M KOH to a new equilibrium state at T_4.

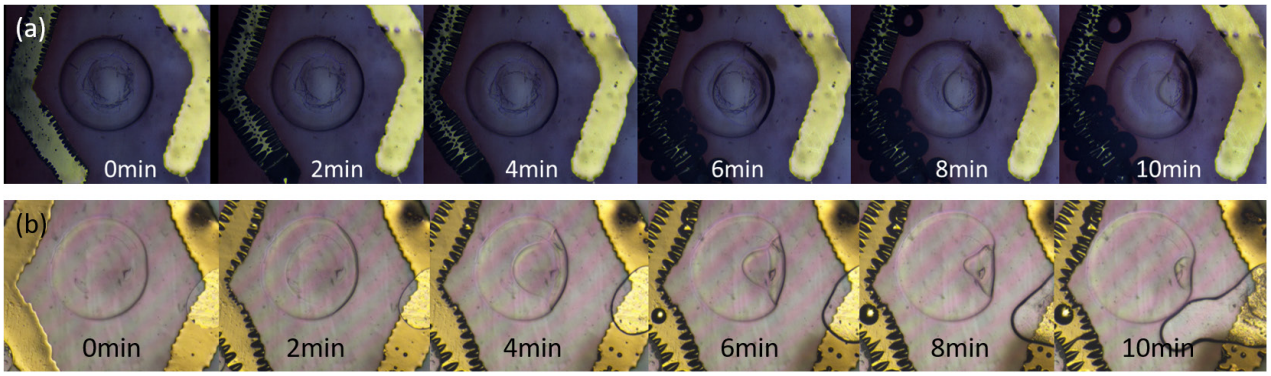

Figure 7. Time profile of deformation induced in two circular hydrogel samples by application of a 2.5 V DC potential between printed Au electrodes. Both samples shrink at anode side and swell at cathode side. (a) Observable hydrogen gas bubbles at cathode. (b) Observable oxygen gas bubble generated at anode.

visible. Quantification of the changing ion concentration could instead be performed by integrating extended gate ion-sensitive field-effect transistors into the channel. It is worth noting that the hydrogel samples behaved similarly when actuated with thin Pt wires in close proximity to the gel samples as when actuated with printed Au electrodes, suggesting that local pH changes can be induced by the printed Au electrodes.

This work demonstrates the feasibility of integrating flexible electronics and electroactive hydrogels within microfluidic channels and suggests that the mechanism for hydrogel deformation observed in this system is electrochemical. The technology can be applied to a range of photo-defineable pH-responsive polymers and printed electroed configurations. Future applications include miniature electro-responsive hydrogel based drug delivery systems, catheter positioning systems, smart implants and systems for performing single cell analysis. For the latter application, producing small forces using a material, hydrogel, that is more mechanically similar to biological cells would be attractive for mechanobiological studies, although a step of insulation cells from local changes of pH and electric fields would be required which is beyond the scope of this work.

4. Conclusions

We have demonstrated morphological manipulation of polyelectrolyte hydrogel microstructures, fabricated *in situ* via single-layer optofluidic lithography, by applying an electrical voltage across printed electrodes, integrated within a microfluidic channel. We proposed that the observed actuation is due to electrochemically-generated pH variation across a hydrogel sample. To address the electrochemical stability of the inkjet-printed electrodes, we determined the stable range using CV in biocompatible buffers.

This work was performed toward integrating EAP hydrogels with MEMS, but further work is required to understand the mechanisms behind EAP actuation and, in turn, optimize hydrogel actuator performance. With improved integration of hydrogels with microfluidics and microelectronics, hydrogel actuators can realize important applications in diagnostics, drug delivery, and on-chip sorting applications. Demonstrating a downscaled hydrogel actuator with integrated printed electronics in microfluidics brings us close to these applications by providing a platform for rapid prototyping of electrode-EAP configurations at low cost which can lead to developing a deeper understanding the role of electrode configuration on the mechanical response of EAP hydrogels to electrical stimulation.

Acknowledgments

This research was partially funded by the Raymond and Beverly Sackler Fund for Convergence Research at Tel Aviv University and UC Berkeley.

This work was partially funded by FlexTech under contract AFOSR-42299 and NSF under contract 1610899.

ORCID iDs

Leeya Engel https://orcid.org/0000-0002-5329-4300
Yasser Khan https://orcid.org/0000-0003-2290-0854
Slava Krylov https://orcid.org/0000-0003-3759-6808

References

[1] Shiga T, Hirose Y, Okada A and Kurauchi T 1994 Deformation of ionic polymer gel films in electric fields *J. Mater. Sci.* **29** 5715–8
[2] Horkay F, Tasaki I and Basser P 2000 Osmotic swelling of polyacrylate hydrogels in physiological salt solutions *Biomacromolecules* **1** 84–90
[3] Rivest C, Morrison D, Ni B, Rubin J, Yadav V, Mahdavi A, Karp J and Khademhosseini A 2007 Microscale hydrogels for medicine and biology: synthesis, characteristics and applications *J. Mech. Mater. Struct.* **2** 1103–19
[4] Lim H, Chuang J, Tran T, Aung A, Arya G and Varghese S 2011 Dynamic electromechanical hydrogel matrices for stem cell culture *Adv. Funct. Mater.* **21** 55–63
[5] Jackson N *et al* 2015 A cardiovascular occlusion method based on the use of a smart hydrogel *IEEE Trans. Biomed. Eng.* **62** 399–406
[6] Jo C, Naguib H and Kwon R 2011 Fabrication, modeling and optimization of an ionic polymer gel actuator *Smart Mater. Struct.* **20** 045006
[7] Kim S, Yoon S, Lee S, Lee S and Kim S 2004 Electrical sensitivity behavior of a hydrogel composed of polymethacrylic acid/poly (vinyl alcohol) *J. Appl. Polym. Sci.* **91** 3613–7
[8] Osada Y, Okuzaki H and Hori H 1992 A polymer gel with electrically driven motility *Nature* **355** 242–4
[9] Bar-Cohen Y and Zhang Q 2008 Electroactive polymer actuators and sensors *MRS Bull.* **33** 173–81
[10] Doi M, Matsumoto M and Hirose Y 1992 Deformation of ionic polymer gels by electric fields *Macromolecules* **25** 5504–11
[11] Wallmersperger T and Ballhause D 2008 Coupled chemo-electro-mechanical finite element simulation of hydrogels: Ii. Electrical stimulation *Smart Mater. Struct.* **17** 045012
[12] He T, Li M and Zhou J 2012 Modeling deformation and contacts of ph sensitive hydrogels for microfluidic flow control *Soft Matter* **8** 3083–9
[13] Harmon M E, Tang M and Frank C W 2003 A microfluidic actuator based on thermoresponsive hydrogels *Polymer* **44** 4547–56
[14] Guo B, Finne-Wistrand A and Albertsson A-C 2011 Degradable and electroactive hydrogels with tunable electrical conductivity and swelling behavior *Chem. Mater.* **23** 1254–62
[15] Richter A, Kuckling D, Howitz S, Gehring T and Arndt K 2003 Electronically controllable microvalves based on smart hydrogels: magnitudes and potential applications *J. Microelectromech. Syst.* **12** 748–53
[16] Kwon G, Choi Y, Park J, Woo D, Lee K, Kim J and Lee S 2010 Electrically-driven hydrogel actuators in microfluidic channels: fabrication, characterization, and biological application *Lab Chip* **10** 1604–10
[17] Beebe D J, Moore J S, Bauer J M, Yu Q, Liu R H, Devadoss C and Jo B-H 2000 Functional hydrogel structures for autonomous flow control inside microfluidic channels *Nature* **404** 588–90
[18] Kim S M *et al* 2013 Stimuli-responsive hydrogel patterns for smart microfluidics and microarrays *Analyst* **138** 6230–42
[19] Kwon G H, Park J Y, Kim J Y, Frisk M L, Beebe D J and Lee S-H 2008 Biomimetic soft multifunctional miniature aquabots *Small* **4** 2148–53
[20] Jackson N and Stam F 2015 Optimization of electrical stimulation parameters for electro-responsive hydrogels for biomedical applications *J. Appl. Polym. Sci.* **132** 41687
[21] Glazer P, van Erp M, Embrechts A, Lemay S and Mendes E 2012 Role of pH gradients in the actuation of electro-responsive polyelectrolyte gels *Soft Matter* **8** 4421–6
[22] Engel L, Berkh O, Adesanya K, Shklovsky J, Vanderleyden E, Dubruel P, Shacham-Diamand Y and Krylov S 2014 Actuation of a novel pluronic-based hydrogel: electromechanical response and the role of applied current *Sensors Actuators* B **191** 650–8
[23] Guan T, Godts F, Ceyssens F, Dubruel P, Neves H and Puers R 2012 Development and fabrication of a novel photopatternable electric responsive pluronic hydrogel for mems applications *Sensors Actuators* A **186** 184–90
[24] Singh M, Haverinen H M, Dhagat P and Jabbour G E 2010 Inkjet printing-process and its applications *Adv. Mater.* **22** 673–85
[25] Pavinatto F J, Paschoal C W and Arias A C 2015 Printed and flexible biosensor for antioxidants using interdigitated ink-jetted electrodes and gravure-deposited active layer *Biosens. Bioelectron.* **67** 553–9
[26] Perelaer J, Smith P J, Mager D, Soltman D, Volkman S K, Subramanian V, Korvink J G and Schubert U S 2010

Printed electronics: the challenges involved in printing devices, interconnects, and contacts based on inorganic materials *J. Mater. Chem.* **20** 8446–53
[27] Khan Y, Pavinatto F J, Lin M C, Liao A, Swisher S L, Mann K, Subramanian V, Maharbiz M M and Arias A C 2016 Inkjet-printed flexible gold electrode arrays for bioelectronic interfaces *Adv. Funct. Mater.* **26** 1004–13
[28] Khan Y *et al* 2016 Flexible hybrid electronics: direct interfacing of soft and hard electronics for wearable health monitoring *Adv. Funct. Mater.* **26** 8764–75
[29] Sochol R D, Casavant B P, Dueck M E, Lee L P and Lin L 2011 A dynamic bead-based microarray for parallel dna detection *J. Micromech. Microeng.* **21** 054019
[30] Schreyer H B, Gebhart N, Kim K J and Shahinpoor M 2000 Electrical activation of artificial muscles containing polyacrylonitrile gel fibers *Biomacromolecules* **1** 642–7
[31] Conway B E and Novak D M 1979 Chloride ion adsorption effects in the recombination-controlled kinetics of anodic chlorine evolution at pt electrodes *J. Chem. Soc. Faraday Trans.* **75** 2454–72
[32] Bianchi G 1971 Fundamental and applied aspects of the electrochemistry of chlorine *J. Appl. Electrochem.* **1** 231–43
[33] Randles J E B 1947 Kinetics of rapid electrode reactions *Discuss. Faraday Soc.* **1** 11–9
[34] Bassil M, Tahchi M E, Souaid E, Davenas J, Azzi G and Nabbout R 2008 Electrochemical and electromechanical properties of fully hydrolyzed polyacrylamide for applications in biomimetics *Smart Mater. Struct.* **17** 055017
[35] Bassil M, Davenas J and Tahchi M E 2008 Electrochemical properties and actuation mechanisms of polyacrylamide hydrogel for artificial muscle application *Sensors Actuators* B **134** 496–501